Regular networks of Luttinger liquids

K. Kazymyrenko and B. Douçot
Laboratoire de Physique Théorique et Hautes Énergies, CNRS UMR 7589, Université Paris VI and VII, 4 Place Jussieu, 75252 Paris Cedex 05, France
(Received 10 July 2004; revised manuscript received 12 October 2004; published 17 February 2005)

We consider arrays of Luttinger liquids, where each node is described by a unitary scattering matrix. In the limit of small electron-electron interaction, we study the evolution of these scattering matrices as the high-energy single particle states are gradually integrated out. Interestingly, we obtain the same renormalization group equations as those derived by Lal, Rao, and Sen, for a system composed of a single node coupled to several semi-infinite one-dimensional wires. The main difference between the single node geometry and a regular lattice is that in the latter case, the single particle spectrum is organized into periodic energy bands, so that the renormalization procedure has to stop when the last totally occupied band has been eliminated. We therefore predict a strongly renormalized Luttinger liquid behavior for generic filling factors, which should exhibit power-law suppression of the conductivity at low temperatures $E_F/(k_F a) \ll k_B T \ll E_F$, where a is the lattice spacing and $k_F a \gg 1$. At lower temperatures $[k_B T \ll E_F/(k_F a)]$, a regular network is generally a coherent conductor, but with a much lower Fermi velocity than for a noninteracting electron gas. Some fully insulating ground states are expected only for a discrete set of integer filling factors for the electronic system. A detailed discussion of the scattering matrix flow and its implication for the low energy band structure is given on the example of a square lattice.

DOI: 10.1103/PhysRevB.71.075110 PACS number(s): 71.10.Pm, 72.10.Fk, 73.21.Hb, 73.23.Ad

I. INTRODUCTION

For the past two decades, transport properties of quantum wires have received a lot of attention.[1,2] Besides metallic systems, two-dimensional electron gases induced in GaAs/AlGaAs heterostructures have displayed a rich variety of quantum effects such as Aharonov-Bohm resistance oscillations in a ring geometry,[3,4] and persistent currents.[5,6] Since the electronic transport mean free path in such artificial nanostructures can be as large as several micrometers, most scattering processes for electronic quasiparticles occur at the nodes between several conducting wires. Their influence has been extensively studied in the context of the breakdown of the quantum Hall effect in narrow channels. Experiments have revealed that the Hall resistance measured in a four probe geometry disappears at low magnetic fields.[7,8] Theoretical studies have emphasized the role of quantum mechanical resonances in the scattering amplitudes of electrons at the junctions between the main channel and voltage probes.[9,10] In experimental systems, confining potentials remain smooth in the vicinity of such junctions, and this induces a rather robust collimation mechanism for incoming electrons.[11,12] This semiclassical picture has been confirmed by spectacular experiments involving junctions with various shapes.[13] More recently, coherent Aharonov-Bohm oscillations have been measured in ballistic arrays with the dice lattice geometry,[14] in agreement with the predictions of simple models for noninteracting electrons.[15,16]

In parallel to this mostly single electron physics, dramatic electron-electron interaction effects have been demonstrated in transport measurements on various ballistic conductors with very few transverse conduction channels. For instance, tunneling into edges of a two-dimensional electronic droplet in the fractional quantum hall effect (FQHE) regime has shown current versus voltage curves with power law behavior[17] in qualitative (though not really quantitative) agreement with theoretical models based on the chiral Luttinger liquid picture.[18] Measurements of shot noise associated to tunneling processes from one edge to another through a quantum point contact have also provided a convincing demonstration of the presence of fractionally charged quasiparticles in the FQHE phase.[19–21] Another family of one-dimensional quantum conductors are carbon nanotubes. In particular, single wall nanotubes have shown a strong reduction of the single particle density of states at low energies,[22,23] compatible with the Luttinger liquid model.[24,25]

These two main lines of research just outlined can be naturally combined and lead us to consider the subject of networks of interconnected quantum wires, each of them being described as a Luttinger liquid. As a first step in this direction, several systems with nanotube crossings have been synthesized.[26–29] On the theoretical side, many studies of Luttinger liquids crossing at one node are now available,[30–34] including extensions to more complex geometries.[35] In this paper, we consider a regular network of Luttinger liquids. As already mentioned, the main source of electron scattering in ballistic structures arises from the nodes of the network. For noninteracting electrons, these nodes are simply described by a scattering matrix,[36–38] and the full band structure (in the absence of disorder) can be retrieved from the knowledge of this matrix. However, as first shown by Kane and Fisher for a single impurity in a Luttinger liquid, interaction effects induce a variation of the dressed scattering matrix as a function of the incoming electron energy.[39,40] One way to interpret this in physical terms is via the notion of Anderson's orthogonality catastrophe: in the limit of a tunnel barrier, an electron jumping across the barrier leaves a dipolar charged excitation which is very far from any eigenstate of the interacting system. A rather complicated collective relaxation process follows any single electron tunneling event. A re-

markable prediction made in these works is a dramatic qualitative difference between repulsive and attractive interactions. In the former case, the effective impurity potential grows as the typical energy becomes closer to the chemical potential. So a single impurity is sufficient to disconnect completely an infinite Luttinger liquid at $T=0$ for repulsive interactions. Conversely, any static impurity becomes transparent in the low energy limit in the case of attractive interactions.

An appealing picture for these effects has been proposed by Yue, Glazman, and Matveev.[41] They have shown that renormalization of the transmission amplitude may be attributed to scattering of an incoming electron on Friedel density oscillations induced by the scatterer. From this picture, they have developed an alternative renormalization approach, which is perturbative in the electron-electron interaction, but nonperturbative in the strength of the impurity potential. This framework has been used later in references,[32,35] and we shall adopt a similar procedure here. Note that a third type of renormalization scheme, involving the full momentum dependence of the electronic self-energy, has been implemented in a series of papers.[42–44]

The main novel feature in regular arrays in comparison to simpler geometries as a few connected wires is the existence of commensurability effects between the Fermi wavelength of electrons and the lattice period. In a noninteracting electron picture, we expect an energy gap in the spectrum when the average electron number in each unit cell of the lattice is an integer. As we shall see later, the band structure for a two-dimensional network yields a gapped excitation spectrum whenever some integer numbers of bands are filled. For interacting electrons, commensurability effects may also be understood by considering the pattern of Friedel density oscillations. In a one-dimensional geometry, these oscillations exhibit a dominant wave vector equal to $2k_F$, where k_F is the Fermi wave vector for a noninteracting one-dimensional wire with the same electronic density. Let us denote by a the distance between two nodes. Friedel oscillations originating from different nodes share the same global phase if $2k_Fa$ is an integer times 2π, which simply means that the average number of electrons along a segment of length a is integer. Therefore, in the case of repulsive interactions, we expect an insulating ground state in the commensurate case, where the Kane-Fisher mechanism will disconnect all the wires incoming at the same node. For incommensurate fillings, we predict a strongly renormalized Fermi liquid, where the partially filled band crossing the Fermi level becomes much less dispersive than for the original noninteracting band structure. We suggest that these effects should be in principle observable in networks of ballistic wires where the electronic density could be controlled by an uniform gate potential. By changing the gate voltage, these systems are expected to undergo a succession of metal-insulator transitions. The difference between an interacting system and a non-interacting one will be manifested by power-law dependences for the conductance as a function of temperature at fixed bias voltage, or as a function of V at fixed T,[39,40] provided both k_BT and eV remain higher than an energy scale Δ which is the renormalized band splitting in the incommensurate case, or the single particle gap in the commensurate one.

This paper is organized as follows: In Sec. II, we consider a simpler problem, namely a one-dimensional chain of regularly spaced impurities. We set up a renormalization group method for weakly interacting electrons which is closely related to those developed in Refs. 32 and 41, but where the periodicity of the system is explicitly taken into account. Section III generalizes this approach to any lattice composed of links of the same length, assumed to be large compared to the Fermi wavelength. We show explicitly that the scattering matrices at each node of such lattices is renormalized exactly in the same way as for a single node connecting semi-infinite wires.[32,41] This is the central result of the present work. As an illustration with possible experimental relevance, Sec. IV considers a two-dimensional square lattice of Luttinger liquids. We show that although the evolution of the scattering matrix of the nodes as the typical energy scale is reduced yields a rather trivial low-energy fixed point where all the links become disconnected, some interesting qualitative changes in the quasiparticle band structure take place along this renormalization group flow.

II. ONE-DIMENSIONAL WIRE WITH A PERIODIC IMPURITY POTENTIAL

The goal of this section is to adapt the simple renormalization group procedure initiated in Refs. 32 and 41 to the case of a periodic potential. The main idea developed in these works is to dress the bare scattering amplitude by a correction due to the interaction of an incoming electron with the Friedel density oscillation induced by the impurity. This approach treats the electron-electron interaction as the perturbation. Because the continuous spectrum of particle-hole excitations in the metallic wire exhibits a finite density of states down to arbitrary low energy, the first order correction to the scattering amplitude diverges as $\ln(|k-k_F|d)$, where k is the incoming electron's wave vector, and d is the spacial range of the bare impurity potential. This type of infrared divergence is very similar to those encountered in the Kondo problem, and Yue *et al.* proposed to treat them with a renormalization group method inspired by Anderson's "*poor man's scaling*" approach.[45] The idea is to integrate out gradually single particle-hole excitations which participate in the Friedel oscillation, starting from those furthest from the Fermi level. As the electron bandwidth D is continuously reduced, the bare impurity potential is renormalized so that the low energy physical properties of the system are kept unchanged. The renormalization procedure stops at a low energy scale with is the larger scale among the thermal broadening k_BT, the bias voltage eV, or the incoming electron energy $\hbar|k-k_F|v_F$.

As already stated in the Introduction, the presence of an array of scattering centers (such as nodes in a wire network) brings qualitatively new features. In the low energy regime, Friedel oscillations originating from different centers are expected to interfere, so we cannot follow the renormalization flow obtained in Refs. 32 and 41 for a single scatterer down to arbitrary low energies. Furthermore, commensuration effects between the average electronic density and the superlattice structure play a crucial role. By contrast to the single

impurity case, we expect an insulating ground-state only for an integer average filling of each supercell. For incommensurate filling factors, we expect a crossover from the one-dimensional behavior following Kane and Fisher's predictions at high energy, towards a strongly renormalized coherent conductor at low energy with finite conductance. The formation of these conducting states in a regular array is analogous to transmission resonances of a single wire in the presence of a finite number of impurities.[40] Whereas the resonant energies form a discrete set in the latter case, they accumulate along finite energy intervals (the Bloch energy bands) for an infinite regular array of impurities.

In a periodic system, the natural way to implement this "*poor man's scaling*" approach is to integrate out energy bands one after the other, starting from those most remote from the Fermi level. In the incommensurate case, the last band, which crosses the Fermi level is partially filled, so it is natural to stop the procedure after the last fully occupied band has been integrated out. In any renormalization method, we have to decide which low-energy quantities will be required to remain constant as high energy modes are eliminated. In the presence of a periodic potential, it is natural to prescribe that single quasiparticle energies should not change under the renormalization group flow (RGF).

A. Band structure for a periodic array of point scatterers

Let us first consider a noninteracting problem along an infinite one-dimensional wire with a periodic potential. The corresponding Hamiltonian is

$$\hat{H} = \frac{\hat{p}^2}{2m} + \sum_{n=0}^{N-1} V(x - na), \tag{1}$$

where a denotes the spacial period of the potential, namely the distance between two succesive impurities. $V(x)$ is a localized potential, so for instance we impose that $V(x)=0$ when $|x|$ is larger than a range d, $d \ll a$. The effect of each scatterer is described by a scattering matrix $\hat{S}$. Suppose first we have only one of them, centered at the origin $x=0$. Let us consider scattering states with the energy $E_0(k)=\hbar^2k^2/(2m)$, k being positive. Away from the impurity, that is for $|x|>d$, we may represent the corresponding wave function as a superposition of plane-waves, see Fig. 1:

$$\psi(x) = \begin{cases} Ae^{ikx} + Be^{-ikx} & \text{for } x < -d \\ A'e^{ikx} + B'e^{-ikx} & \text{for } x > d. \end{cases} \tag{2}$$

Since Schrödinger's equation is linear and of second order, we may express the outgoing amplitudes A' and B linearly as a function of the incoming ones A and B'

$$\begin{pmatrix} A' \\ B \end{pmatrix} = \begin{pmatrix} t & r' \\ r & t' \end{pmatrix} \begin{pmatrix} A \\ B' \end{pmatrix} \equiv \hat{S} \begin{pmatrix} A \\ B' \end{pmatrix}, \tag{3}$$

where $\{r,t,r',t'\}$ are two pairs of reflection and transmission coefficients for left and right sides of the node. In principle, these four coefficients do depend on the energy of the particle or equivalently on its wave vector k. In this paper, we shall neglect this variation, since the dominant contribution

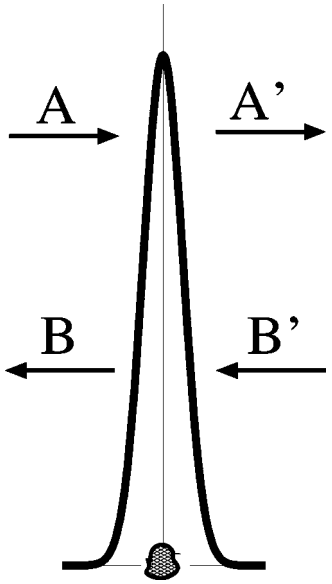

FIG. 1. Localized impurity potential may be represented by an $\hat{S}$ matrix that connects amplitudes of incoming (A,B') and outgoing (A',B) plane waves outside the impurity.

processes involve virtual excitation of particle-hole pairs in the vicinity of the Fermi level. A more complete approach would consider the Taylor expansion of $\hat{S}$ in powers of $k - k_F$, but all terms beyond the 0th order one are irrelevant according to the classification of perturbations around a noninteracting one-dimensional fermion system. At least for not too large interactions, they are not supposed to change the qualitative picture of the system behavior. As usual, this $\hat{S}$ matrix is unitary. Assuming time reversal invariance of the Hamiltonian implies $t=t'$ and if $V(x)$ is an even function of x, we have also $r=r'$. In this case, we may parametrize $\hat{S}$ by two angles $(0 \leqslant \phi \leqslant \pi/2,\ 0 \leqslant \psi < 2\pi)$

$$\hat{S} = e^{i\psi} \begin{pmatrix} \cos\phi & \pm i \sin\phi \\ \pm i \sin\phi & \cos\phi \end{pmatrix}. \tag{4}$$

For a periodic array of identical scatterers, eigenstates may be obtained as Bloch functions, namely we may impose the condition

$$\psi(x + a) = e^{ik'a}\psi(x),$$

where k' is chosen in the first Brillouin zone $[-\pi/a, \pi/a]$. On each x interval $[na+d,(n+1)a-d]$, we write the eigenstate with energy $E_0(k)$ as

$$\psi(x) = A_n e^{ikx} + B_n e^{-ikx}.$$

The above periodicity condition implies

$$A_n = e^{i(k'-k)an} A_0,$$

$$B_n = e^{i(k'+k)an} B_0.$$

Equation (3) can now be written for each impurity site, which gives

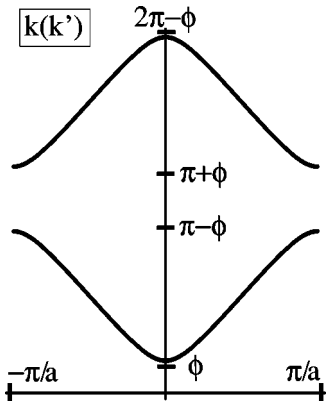

FIG. 2. Band structure for 1D wire of noninteracting electrons with periodic impurities. BS is 2π periodic in k. A set of gaps $(-\phi+2\pi n, \phi+2\pi n)$ and $(\pi-\phi+2\pi n, \pi+\phi+2\pi n)$ is present for any value of the $\hat{S}$ matrix.

$$\begin{pmatrix} A_{n+1}e^{ika(n+1)} \\ B_n e^{-ika(n+1)} \end{pmatrix} = \begin{pmatrix} t & r' \\ r & t' \end{pmatrix} \begin{pmatrix} A_n e^{ika(n+1)} \\ B_{n+1}e^{-ika(n+1)} \end{pmatrix}. \tag{5}$$

Replacing A_n and B_n by their expressions in terms of A_0 and B_0, we get the following secular equation:

$$\begin{vmatrix} te^{i(k-k')a} - 1 & r' \\ re^{i2ka} & t'e^{i(k+k')a} - 1 \end{vmatrix} = 0 \tag{6}$$

which determines the dispersion relation implicitly via k, the energy being $E_0(k)$, the lattice momentum k' behaving as an external parameter. Using a normalization condition on the wave function, we could get (A_0, B_0) as functions of $(k', \hat{S})$.

In the particular case of spacially even and time-reversal invariant potentials, we may use the above parametrization for $\hat{S}$ in Eq. (6), which yields

$$\cos(ka + \psi) = \cos\phi \cos(k'a). \tag{7}$$

For a given value of the lattice momentum k', the possible values of ka appear in two equally spaced families, with a period 2π for each of them. The allowed values of $ka+\psi$ belong to the intervals $[-\pi+\phi+2\pi n, -\phi+2\pi n]$ and $[\phi+2\pi n, \pi-\phi+2\pi n]$, where n is an integer. We recall that k should be *positive*, in order not to count each eigenstate twice. The values of $ka+\psi$ lying in intervals $[-\phi+2\pi n, \phi+2\pi n]$, and $[\pi-\phi+2\pi n, \pi+\phi+2\pi n]$ correspond then to energy gaps. These gaps are of course larger when the reflexion coefficient is larger, see Fig. 2.

For a noninteracting electron system, the Fermi sea contains an integer number n of filled bands whenever the average electronic density corresponds exactly to n electrons per unit cell. For generic filling factors, the Fermi level crosses a partially filled band for a lattice momentum k'_F. The corresponding Fermi group velocity is then

$$v_F^{*(0)} = v_F \frac{dk}{dk'}(k'_F) = v_F \frac{\cos\phi |\sin(k'_F a)|}{\sqrt{1 - \cos^2\phi \cos^2(k'_F a)}}, \tag{8}$$

where $v_F = \hbar k_F / m$ is the Fermi velocity of a uniform noninteracting gas with the same density.

B. Switching on electron-electron interactions

In a Luttinger liquid, the effective interaction becomes non-local in the low-energy limit. To show this, it is convenient to decompose the electron creation operators $\Psi^+_\sigma(x)$ (where $\sigma \in \{\uparrow, \downarrow\}$ denotes the spin component along a fixed direction) into a right moving part $\Psi^+_{R\sigma}(x)$ and a left-moving part $\Psi^+_{L\sigma}(x)$, where $\Psi^+_{R\sigma}$ ($\Psi^+_{L\sigma}$) involves the Fourier modes k close to k_F ($-k_F$). With this decomposition, the local electron density $\rho(x)$ is written as follows:

$$\begin{aligned} \rho(x) &= \sum_{\sigma=\uparrow,\downarrow} \Psi^+_\sigma(x)\Psi_\sigma(x) \\ &= \sum_{\sigma=\uparrow,\downarrow} [\Psi^+_{R\sigma}(x)\Psi_{R\sigma}(x) + \Psi^+_{L\sigma}(x)\Psi_{L\sigma}(x)] \\ &\quad + \sum_{\sigma=\uparrow,\downarrow} [\Psi^+_{R\sigma}(x)\Psi_{L\sigma}(x) + \Psi^+_{L\sigma}(x)\Psi_{R\sigma}(x)]. \end{aligned} \tag{9}$$

The first two terms are smooth fields, meaning that their Fourier transforms involve only small wave vectors compared to k_F. But the last two terms are centered around the wave vectors $\pm 2k_F$ so they are rapidly oscillating. For a spin-rotation invariant Hamiltonian, the effective low energy description of a Luttinger liquid involves three independent parameters: the velocities v_c and v_s of collective charge and spin excitations, and a dimensionless constant K which depends on the strength of electron-electron interactions and controls the exponents entering the correlation functions. Since transport properties are mostly affected by the value of K,[39] we shall not consider here the renormalizations of v_c and v_s away from their common value v_F for a noninteracting system. Therefore, it is sufficient to consider the following interaction:

$$H_{\text{int}} = \frac{U_0}{2} \int_{-L/2}^{L/2} dx \rho_0(x)^2, \tag{10}$$

where $\rho_0(x)$ is the long wavelength part of the total density:

$$\rho_0(x) = \sum_{\sigma=\uparrow,\downarrow} [\Psi^+_{R\sigma}(x)\Psi_{R\sigma}(x) + \Psi^+_{L\sigma}(x)\Psi_{L\sigma}(x)].$$

Here L denotes the total length of the system. Later, we shall assume periodic boundary conditions, and that L encloses an integer number N of periodic cells, so $L=Na$. With this choice of interaction, we have

$$v_c = v_F \left(1 + \frac{2U_0}{\pi\hbar v_F}\right)^{1/2},$$

$$v_s = v_F,$$

$$K = \left(1 + \frac{2U_0}{\pi\hbar v_F}\right)^{-1/2}.$$

So $K=1$ for a noninteracting system, $K>1$ for attractive interactions, and $K<1$ for repulsive interactions. For our purpose, it is convenient to view this effective interaction as deriving from a *nonlocal* potential $U(x-y)$ such that its Fourier transform $\tilde{U}(k)$ vanishes outside a finite window cen-

tered around $k=0$ and whose width is smaller than $2k_F$. The interaction strength U_0 is defined as $\tilde{U}(k=0)$. With this notation, we have

$$H_{\text{int}} = \frac{1}{2}\int_{-L/2}^{L/2} dx \int_{-L/2}^{L/2} dy \rho_0(x) U(x-y) \rho_0(y). \qquad (11)$$

In this section, we are considering the combined effect of impurity scattering and interactions. Renormalizations of the effective scattering matrix $\tilde{S}$ are naturally detected via the electron self-energy $\Sigma(k,k',\omega)$. But since our system exhibits only a discrete translation symmetry, we may only conclude that $k'-k$ should be an integer multiple of the basic reciprocal lattice vector $2\pi/a$. This self-energy is then a relatively complicated object. More information on its real-space structure for a single impurity may be found in Refs. 42 and 43. To analyze it in a simple way we shall compute the first order correction $E_1(k)$ with respect to U_0 to the single electron energy $E_0(k)=\hbar^2k^2/(2m)$. Here k stands for a single particle level, close to the Fermi energy, and labelled by the combination of a Bloch quasi-momentum k' and a band index. This correction $E_1(k)$ is given by the sum of a Hartree term and of an exchange term. In the case of an unpolarized electron system, we have

$$E_1(k) = \int_{-L/2}^{L/2} dx \int_{-L/2}^{L/2} dy \sum_{q<k_F} \psi_k^*(x)\psi_q^*(y)U(x-y) \times [2\psi_q(y)\psi_k(x) - \psi_q(x)\psi_k(y)]. \qquad (12)$$

For local potentials, the Hartree and the exchange contributions cancel each other, when the spins of the two electrons involved are parallel. But as we have recalled before, our two-body effective potential is in fact nonlocal, so we have to analyze both terms in more detail. Our expression for $E_1(k)$ involves integrals of the form:

$$I_U(f,g) = \int_{-L/2}^{L/2} dx \int_{-L/2}^{L/2} dy f^*(x) U(x-y) g(y)$$

where $f(x)$ and $g(y)$ are Bloch functions satisfying

$$\frac{f(x+a)}{f(x)} = \frac{g(y+a)}{g(y)} = e^{i\theta}, \quad 0 < \theta \leqslant 2\pi.$$

Since U is short-ranged in space (though it is *not* a delta function), we may take safely the thermodynamic limit $L \to \infty$. Writing $f(x)=\Sigma_n \tilde{f}_n e^{i(2\pi n+\theta)x/a}$ and an analogous series for $g(y)$, we obtain

$$I_U(f,g) = L\sum_n \tilde{f}_n^* \tilde{U}\left(\frac{2\pi n+\theta}{a}\right)\tilde{g}_n \simeq LU_0 \sum_{|n|\ll k_F a} \tilde{f}_n^* \tilde{g}_n. \qquad (13)$$

Let us first consider the Hartree term. Because we chose single particle eigenstates of the Bloch form, the corresponding local particle density is periodic with period a. A little elementary algebra shows that

$$|\psi_k(x)|^2 = \frac{1}{Na} \frac{\sin(ka+\psi) \pm \sin(\phi)\cos\left[2k\left(x-\frac{a}{2}\right)\right]}{\sin(ka+\psi) \pm \sin(\phi)\sin(ka)/(ka)} \qquad (14)$$

for $0<x<a$. As expected, the amplitude of the local density oscillation is stronger when the bare reflexion coefficient is larger, or equivalently when $|\sin(\phi)|$ is larger. The nth Fourier amplitude of this local density is equal (for $n \neq 0$) to:

$$\frac{\mathcal{A}_k}{2Na}\left(\frac{\sin(ka-\pi n)}{ka-\pi n} + \frac{\sin(ka+\pi n)}{ka+\pi n}\right),$$

where the numerical coefficient $\mathcal{A}_k$ is close to unity. As shown in Eq. (13) above, we are interested in the case where $|n| \ll k_F a$, and since k is close to k_F, this amplitude is small by a factor $1/(k_F a)$. A similar conclusion holds for the Fourier amplitudes of $|\Psi_q(x)|^2$ if we assume that the most important effects come from filled states where q is close to k_F. Therefore, we do not expect strong renormalizations coming from the Hartree term.

Let us now turn to the exchange term. The product $\Psi_q^*(y)\Psi_k(y)$ is the sum of four oscillating terms proportional to $e^{\pm i(k-q)y}$ and $e^{\pm i(k+q)y}$. The last two terms are fast oscillations which will be filtered out by the nonlocal potential, as in Eq. (13). Keeping only the first two oscillations, we can cast the exchange contribution to $E_1(k)$ as follows:

$$E_1(k) = c\frac{U_0}{a}(k_F' + N_F\pi) - \frac{U_0}{2\pi a}\sin^2\phi \int \frac{dq'}{\sin(k+\psi)\sin[q(q')+\psi]} \times \frac{\sin[q(q')-k]}{q(q')-k}. \qquad (15)$$

In this equation, we have replaced combinations such as ka, qa, by new dimensionless variables k, q. The integral symbol stands for a summation over all the N_F completely filled bands, including possibly a last partially filled band with a dimensionless momentum k_F' such that $0 \leqslant k_F' < \pi$. For each completely filled band, the integration variable q' runs from 0 to π, and q in Eq. (15) is a function of the lattice momentum q' solution of the dispersion relation (7). For the last partially filled band (incommensurate case), the q' integral runs from 0 to k_F'. As already mentioned, we have assumed that parameters (ψ,ϕ) are not depending on the incoming energy. Note that contributions from the Hartree term will modify only the numerical coefficient c whose precise value is not important here.

C. Renormalization approach

Let us introduce the notation $\Lambda_0=\pi N_F$, which plays the role of a large momentum cut-off. As in all schemes inspired by Anderson's "*poor man's scaling*," we shall assume it is possible to construct a sequence of models where filled bands are eliminated one after the other, starting from the most remote from the Fermi level. When the first n bands

have been eliminated, the new value of Λ is set equal to $\Lambda_0 - \pi n$. At each step, we require that the quasiparticle energy $[E_{\rm tot}(k)=E_0(k)+E_1(k)\equiv E_0(k)+U_0\mathcal{E}_1(k)]$ for k close to the Fermi wave vector should remain unchanged. To compensate for the reduction of the cut-off from Λ_0 to Λ, we have to adjust $\hat{S}$-matrix parameters $\{\psi,\phi\}$ so they become functions of running cutoff Λ. This is expressed by the following prescription:

$$E_{\rm tot}(\psi_0,\phi_0,k) = E_0\big(\psi(\Lambda),\phi(\Lambda),k\big) + U_0\mathcal{E}_1\big(\psi(\Lambda),\phi(\Lambda),k,\Lambda\big). \tag{16}$$

Since for $U_0=0$, this condition implies $E_0(\psi_0,\phi_0,k) = E_0\big(\psi(\Lambda),\phi(\Lambda),k\big)$, we see that in this case $(\psi_0,\phi_0) = \big(\psi(\Lambda),\phi(\Lambda)\big)$ for any Λ, so we may write the following Taylor series:

$$\psi(\Lambda,U_0,\psi_0,\phi_0,\Lambda_0) \equiv \psi_0 + U_0\overline{\psi}(\Lambda,\psi_0,\phi_0,\Lambda_0) + O(U_0^2),$$

$$\phi(\Lambda,U_0,\psi_0,\phi_0,\Lambda_0) \equiv \phi_0 + U_0\overline{\phi}(\Lambda,\psi_0,\phi_0,\Lambda_0) + O(U_0^2).$$

We now try to keep band structure (16) unchanged for any k

$$\begin{aligned} &E_0(\psi_0,\phi_0,k) + U_0\mathcal{E}_1(\psi_0,\phi_0,k,\Lambda_0) \\ &\quad = E_0\big(\psi_0 + U_0\overline{\psi}(\Lambda),\phi_0 + U_0\overline{\phi}(\Lambda),k\big) \\ &\qquad + U_0\mathcal{E}_1\big(\psi_0 + U_0\overline{\psi}(\Lambda),\phi_0 + U_0\overline{\phi}(\Lambda),k,\Lambda\big). \end{aligned}$$

Keeping the first order terms in U_0 gives

$$\left.\frac{\partial E_0}{\partial\psi}\right|_{\psi_0}\overline{\psi}(\Lambda) + \left.\frac{\partial E_0}{\partial\phi}\right|_{\phi_0}\overline{\phi}(\Lambda) = \mathcal{E}_1(\psi_0,\phi_0,k,\Lambda_0) - \mathcal{E}_1(\psi_0,\phi_0,k,\Lambda). \tag{17}$$

This is a nontrivial constraint, since $\partial E_0/\partial\psi|_{\psi_0}$ and $\partial E_0/\partial\phi|_{\phi_0}$ depend on k but do not depend on Λ. On the contrary, $\overline{\psi}$ and $\overline{\phi}$ depend on Λ but not on k. The possibility to enforce this requirement is not obvious *a priori*, and when it occurs, we may call our model *renormalizable* (at least to this lowest order).

Let us now evaluate the right-hand side of this equation. Suppose we integrate out just one band, then $\Lambda_0-\Lambda=\pi$, which is assumed to be much smaller than Λ. While computing $\mathcal{E}_1(\psi_0,\phi_0,k,\Lambda_0)-\mathcal{E}_1(\psi_0,\phi_0,k,\Lambda)$ in Eq. (15), the integral involves only one band far from the Fermi level. Therefore, we may further approximate $q(q')-k$ by $-\Lambda$. This yields

$$\mathcal{E}_1(\psi_0,\phi_0,k,\Lambda_0) - \mathcal{E}_1(\psi_0,\phi_0,k,\Lambda) \simeq \frac{c(\Lambda_0-\Lambda)}{a} + \frac{1}{\Lambda}\frac{1}{2\pi a}\frac{\sin^2\phi_0}{\sin(k+\psi_0)}\int_0^\pi dq'\,\frac{\sin[q(q')-k]}{\sin[q(q')+\psi_0]}. \tag{18}$$

From (7) the derivatives involved in the left-hand side of Eq. (17) are

$$\left.\frac{\partial E_0}{\partial\psi}\right|_{\phi,k=\text{const}} \approx -\frac{\hbar v_F}{a},$$

$$\left.\frac{\partial E_0}{\partial\phi}\right|_{\psi,k=\text{const}} \approx \frac{\hbar v_F}{a}\tan\phi\cot(k+\psi).$$

We have linearized the bare dispersion relation: $E_0(k) = \hbar^2k^2/(2ma^2) \approx \text{const} + (\hbar v_F/a)k$. The notation "$k=$const" means more precisely that the Bloch crystal momentum k' and the band index have to be maintained constant while varying ϕ or ψ. Introducing these expressions for the derivatives and the result (18) in Eq. (17) shows that indeed the k dependencies on both sides can be made to match, which expresses the renormalizability of our model to first order in interaction strength. This fixes the form of the functions $\overline{\psi}(\Lambda)$ and $\overline{\phi}(\Lambda)$:

$$\overline{\psi}(\Lambda,\psi_0,\Lambda_0) = \frac{1}{\hbar v_F}\left(c(\Lambda-\Lambda_0) - \frac{\sin^2\phi_0}{2\pi}\ln\frac{\Lambda}{\Lambda_0}\int_0^\pi dq'\,\cot[q(q')+\phi_0+\psi_0]\right),$$

$$\overline{\phi}(\Lambda,\phi_0,\Lambda_0) = -\frac{1}{4\pi\hbar v_F}\sin(2\phi_0)\ln\frac{\Lambda}{\Lambda_0}.$$

Finally we construct the RGF equation:

$$\frac{\partial\psi}{\partial\Lambda} = \frac{U_0}{\pi\hbar v_F}\left(c + \frac{\sin^2\phi}{2\pi}\frac{1}{\Lambda}\int_0^\pi dq'\,\cot[q(q')+\psi]\right), \tag{19}$$

$$\frac{\partial\phi}{\partial\ln\Lambda} = -\frac{U_0}{4\pi\hbar v_F}\sin 2\phi. \tag{20}$$

We see from Eq. (4) that the parameter ψ is a global phase in the scattering matrix, which does not affect any physical property of the system besides an overall shift of the single particle spectrum. In particular, it does not generate any density oscillation. Moreover the associated RGF equation explicitly involves the running cut-off Λ, and the notion of fixed point loses its meaning here.

Therefore, we now turn to $\phi(\Lambda)$, for which a simple RGF equation arises, and which solution is given by

$$\tan\phi = (\Lambda_0/\Lambda)^\alpha\tan\phi_0, \tag{21}$$

where $\alpha=U_0/(2\pi\hbar v_F)$. The corresponding transmission coefficient $T(\Lambda)$ on a given impurity is

$$T(\Lambda) = \cos^2[\phi(\Lambda)] = \frac{T_0(\Lambda/\Lambda_0)^{2\alpha}}{R_0 + T_0(\Lambda/\Lambda_0)^{2\alpha}}, \tag{22}$$

where T_0 is the transmission coefficient for a single impurity in absence of interaction, and $R_0=1-T_0$. This result agrees with the expression obtained for a single impurity[41] in the absence of spin backscattering, namely when $\tilde{U}(2k_F)=0$. Again, this approach assumes small electron-electron interactions. In the case of strong interactions, where K is no longer close to 1, the bosonization method shows that for the single impurity problem, α should be replaced by $(1-K)/2$.[40] These two expressions for the exponent coincide at small U_0 if terms of order U_0^2 or higher are neglected.

For a commensurate system ($k_F a = \pi n$, n integer), the noninteracting ground-state is already gapped, so we expect a true insulator as well in the presence of repulsive interactions. The difference between a traditional band insulator and the one obtained here in the presence of interactions is the nontrivial energy dependence of the impurity scattering matrix and the corresponding behavior of the Landauer conductance, Eq. (22). For an incommensurate system, we have a partially filled band crossing the Fermi level in the absence of interaction. Since our renormalization procedure assumed a gradual elimination of fully occupied bands, it has to break down after the last of those bands has been integrated out. Treating the remaining partially occupied band in a heuristic way, we simply assume that it corresponds to a strongly renormalized Luttinger liquid, whose effective Fermi velocity v_F^* is much reduced compared to the Fermi velocity $v_F = \hbar k_F / m$ of a uniform noninteracting gas with the same density. More precisely, we have, according to Eq. (8):

$$v_F^* \simeq v_F \cos \phi_S \sin(k_F' a),$$

where $\phi_S \simeq \pi/2$ is the value of ϕ when the renormalization procedure stops, which corresponds to

$$\frac{\Lambda_0}{\Lambda} = \frac{k_F a}{\pi}.$$

Note that the denominator in Eq. (8) is then very close to unity. Using Eq. (21), we get

$$v_F^* = v_F \left(\frac{\pi}{k_F a} \right)^{\alpha} \cot \phi_0 \sin(k_F' a). \tag{23}$$

III. GENERALIZATION OF RG PROCEDURE TO A LARGE CLASS OF LATTICES

In the previous section we introduced the main ideas we used to obtain the RGF equation for a 1D lattice. We wish now to show that renormalizability of this particular 1D system is not a simple coincidence, but a general property of any network (not necessarily periodic), provided the two following assumptions hold, namely all the links have the same length, which has to be large compared to the Fermi wavelength. Let us begin to follow the same procedure as in one dimension. Suppose that we have a network of equal length wires. Any junction point is described by an unitary $\hat{S}$ matrix which dimension is equal to the number of wires joining at this node. For each link, stationary single electron states can be written as the sum of two plane waves,

$$\psi(x) = A_{ij} e^{-ikx} + A_{ji} e^{ikx}, \tag{24}$$

where A_{ij} is the amplitude of the wave that propagates from node j to node i, if the x coordinate is oriented from i to j. Solving Schrödinger's equation is equivalent to connect these various amplitudes via node scattering matrices

$$A_{ij} = \sum_m {}^{(j)} e^{ika} S_{im}^{(j)} A_{jm}. \tag{25}$$

Here $\Sigma_m^{(j)}$ means that we sum over first neighbors m of node j. We notice that this has indeed the form of an eigenvalue equation written in some basis. Following the idea of Kottos and Smilansky[46] we introduce a finite dimensional Hilbert space associated to the lattice links. Each link ij is represented by two orthonormal vectors $|ij\rangle$ and $|ji\rangle$. The dimension of this auxiliary Hilbert space is therefore $2N_L$ (N_L is the total number of links). One may rewrite Eq. (25) in its vector form

$$\hat{T}|A(k)\rangle = e^{-ika}|A(k)\rangle, \tag{26}$$

where the $\hat{T}$ operator incorporates information about the scattering matrices of all nodes,

$$\hat{T} = \sum_j \sum_{i,m} {}^{(j)} |ij\rangle S_{im}^{(j)} \langle jm| \Leftrightarrow S_{im}^{(j)} = \langle ij|\hat{T}|jm\rangle. \tag{27}$$

As this operator $\hat{T}$ is unitary and defined in a finite dimensional Hilbert space, it could be diagonalized as $\hat{T}|\alpha\rangle = e^{-i\theta_\alpha}|\alpha\rangle$, where α takes $2N_L$ values and θ_α is real. So we obtain families of eigenvalues for the single electron energy $E = \hbar^2 k^2 / 2m$,

$$a k_{\alpha,n} = \theta_\alpha + 2\pi n \geqslant 0. \tag{28}$$

We emphasize that this periodic structure of the single particle spectrum is a special feature of constant link length networks. A brief discussion of the more general case is given in Appendix C. Because of this periodicity, and despite the absence of any translational symmetry, we may still introduce a notion of energy band for such lattices. More precisely, in this setting, an energy band corresponds to fixing n and allowing for all possible values of θ. Note that this notion of band does not exactly coincide with the more familiar notion from the Bloch theory of translational invariant lattices. For simple Bravais lattices, the number of states in each Bloch band is the number of unit cells which is equal to the number of sites N_S. If Z is the coordination number, we have $ZN_S = 2N_L$, so our generalized bands contain Z usual Bloch bands for a Bravais lattice. At this stage, we have so far a band structure equation written in operator form. In order to obtain renormalization flow for the $\hat{S}$-matrix we need to compute first the electron-electron contribution as in Eq. (12) to the single electron energy and then the variation in the unperturbed energy due to an arbitrary $\hat{S}$-matrix change $\partial E_0 / \partial \hat{S}$.

As in one dimension, the main contribution to the electronic self-energy is given by the exchange term. Let us consider a pair of single particle eigenstates labelled by k and q, where these labels should in fact be viewed as pairs (α, n) and (β, m), m and n being integers according to the above description of the spectrum. State k is close to the Fermi level, but state q is far from it, at a distance corresponding to the current energy cut-off Λ. Along a link ij, we denote by $[\Psi_k^*(x)\Psi_q(x)]_0$ the slowly varying component of $\Psi_k^*(x)\Psi_q(x)$. A simple computation shows that:

$$\frac{1}{L}\int_i^j |[\Psi_k^*(x)\Psi_q(x)]_0|^2 = |A_{ij}(k)|^2|A_{ij}(q)|^2 + |A_{ji}(k)|^2|A_{ji}(q)|^2$$

$$+ [A_{ji}^*(k)A_{ij}(k)A_{ji}(q)A_{ij}^*(q) + \text{H.c.}]\frac{\sin(k-q)L}{(k-q)L}. \quad (29)$$

The first part summed over fully completed band does not depend on energy:

$$\sum_{q\in\text{Band}}\sum_{i,j}|A_{ij}(k)|^2|A_{ij}(q)|^2 + |A_{ji}(k)|^2|A_{ji}(q)|^2$$

$$= \sum_{q\in\text{Band}}\sum_{\langle ij\rangle}|A_{ij}(k)|^2|A_{ij}(q)|^2 = \sum_{\langle ij\rangle}\langle ij|k\rangle\langle k|ij\rangle\langle ij|\sum_{q\in\text{Band}}|q\rangle$$

$$\times\langle q|ij\rangle = \sum_{\langle ij\rangle}\langle k|ij\rangle\langle ij|k\rangle = \langle k|k\rangle = 1. \quad (30)$$

We used the fact that both $|q\rangle$ and $|ij\rangle$ form complete basis sets in our Hilbert space. The main expression to compute is then

$$I(k) = \sum_{q\in\text{Band}}\sum_{\langle jm\rangle}A_{jm}^*(k)A_{mj}(k)A_{jm}(q)A_{mj}^*(q)\sin(k-q)a, \quad (31)$$

where the sum over q is just a single band sum, namely m is fixed, and the sum is taken over the $2N_L$ values of β. The power of this algebraic formalism is that such sum is readily performed, without having to compute any integral. Indeed, we have

$$I(k) = \sum_q\sum_{\langle ij\rangle}\langle k|ij\rangle\langle ij|q\rangle\sin[(k-q)a]\langle q|ji\rangle\langle ji|k\rangle. \quad (32)$$

As shown in Appendix C, we may assume that the eigenvectors $|q\rangle$ are normalized to unity in the auxiliary Hilbert space attached to link amplitudes, provided the links have the same length, much larger than the Fermi wavelength. Therefore, we have the very useful completeness relation, that is

$$\sum_q |q\rangle e^{-iqa}\langle q| = \hat{T}. \quad (33)$$

After some simple algebra, we may cast $I(k)$ into the form

$$I(k) = e^{ika}\frac{i}{\alpha}\langle k|\sum_j\sum_{l,m}{}^{(j)}|lj\rangle V_{lm}^{(j)}\langle jm|k\rangle = e^{ika}\frac{i}{\alpha}\langle k|\hat{\mathbf{V}}|k\rangle, \quad (34)$$

where the single node operators $\hat{V}^{(j)}$ are defined by

$$\hat{V}^{(j)} = \hat{F}^{(j)} - \hat{S}^{(j)}\hat{F}^{(j)\dagger}\hat{S}^{(j)}$$

and the diagonal matrix $\hat{F}^{(j)}$ by

$$F_{ii}^{(j)} = -\tfrac{1}{2}\alpha S_{ii}^{(j)}.$$

We have introduced as before the dimensionless parameter $\alpha = U_0/(2\pi\hbar v_F)$.

To get the first order variation of the single electron energy under small changes in the node scattering matrix parameters we differentiate Eq. (26):

$$(d\hat{T})|k\rangle + \hat{T}|dk\rangle = -i(dk)ae^{-ika}|k\rangle + e^{-ika}|dk\rangle. \quad (35)$$

Applying $\langle k|$ to this equation and using $\langle k|\hat{T} = e^{-ika}\langle k|$ we obtain

$$dk = \frac{i}{a}e^{ika}\frac{\langle k|d\hat{T}|k\rangle}{\langle k|k\rangle}. \quad (36)$$

This allows us to calculate single electron energy variations due to $\hat{S}$-matrix changes. In the particular case of global phase transformation, the corresponding infinitesimal form reads: $d\hat{T} = i\hat{T}d\psi$. Clearly, the energy differential does not depend on energy any more since $dk = -d\psi/a$, so global phase shifts simply induce a global translation on the energy spectrum.

Following the same ideas as in 1D, we generalize the RGF equation to any $\hat{S}$-matrix parametrization. Equation (17) now becomes

$$\frac{\partial E_0}{\partial S}(\hat{S}_0,k)dS(\Lambda) = E_1(\hat{S}_0,k,\Lambda_0) - E_1(\hat{S}_0,k,\Lambda). \quad (37)$$

The left-hand side of this equation is equal to $\hbar v_F dk$, where dk is related to the small renormalization of $\hat{T}$ by Eq. (36). To evaluate right-hand side, as before, we integrate just over one band of width 2π for the quantity $q_{\beta,m}a$, i.e. $d\Lambda = \Lambda - \Lambda_0 = -2\pi$,

$$\hbar v_F dk = E_1(\hat{S}_0,k,\Lambda_0) - E_1(\hat{S}_0,k,\Lambda) = \frac{cU_0(\Lambda_0-\Lambda)}{a}$$

$$-\frac{U_0}{a}\sum_{\Lambda<qa<\Lambda_0}\sum_{\langle jm\rangle}A_{jm}^*(k)A_{mj}(k)A_{jm}(q)A_{mj}^*(q)$$

$$\times\frac{\sin(k-q)a}{(k-q)a} = -\frac{cU_0 d\Lambda}{a} - \frac{U_0}{a}\frac{1}{\Lambda}\left(-\frac{d\Lambda}{2\pi}\right)I(k).$$

Constant c includes both the Hartree term and the part of exchange term that does not depend on k, so we do not precise its value since it renormalizes only the global phase of the $\hat{S}$-matrix.

Finally, we get the result $d\hat{T}/dl = -\hat{\mathbf{V}}$ that agrees completely with Lal, Rao, and Sen,[32] obtained for a single node connecting an arbitrary number of semi-infinite 1D wires. In coordinate way of writing, it gives

$$\frac{d\hat{S}^{(j)}}{dl} = \hat{S}^{(j)}\hat{F}^{(j)\dagger}\hat{S}^{(j)} - \hat{F}^{(j)}, \quad (38)$$

where we just chose the usual cutoff parametrization: $\Lambda = \Lambda_0 e^{-l}$.

IV. TWO-DIMENSIONAL SQUARE LATTICE

We would like to illustrate the result of the previous section on one more example. This part could be interesting from an experimental viewpoint, since present nanofabrication techniques are now available to prepare networks of quantum wires with a very small number of transverse con-

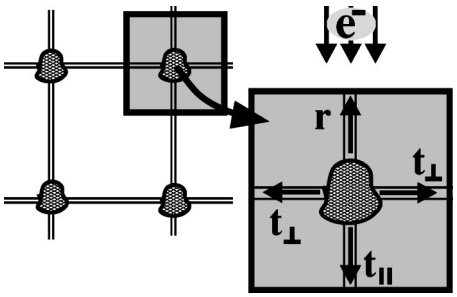

FIG. 3. Two-dimensional periodic grid of electron liquids with impurities. Each impurity could be represented by 3 complex parameters: r, reflection; $t_{\|}$, forward transmission; $t_{\perp}$, perpendicular transmission coefficients.

duction channels etched on a two-dimensional electron gas with high mobility, as illustrated for instance in Ref. 14. Let us now consider an infinite regular square lattice of perfect Luttinger wires. These one-dimensional conductors are only coupled at the lattice nodes which are described by a single 4×4 scattering matrix $\hat{S}$. To keep a simple model, we shall restrict ourselves to the case of a single conduction channel in each wire, although the case of several channels would clearly be of interest, both on the theoretical side, and with respect to possible experimental realizations. As mentioned in the Introduction, we shall not take into account any energy dependence of the scattering matrix, although detailed studies of the Schrödinger equation for a cross of wires with a finite width have exhibited a rich pattern of resonances.[47,48] The main motivation for this simplified treatment is that in a renormalization group picture, smooth energy dependencies in the scattering matrix as a function of $E-E_F$ correspond to irrelevant operators, which should not alter drastically the way interactions drive the system to its low-energy fixed point. Labeling the four directions joining at a node as in Fig. 3, we shall consider a scattering matrix of the following form:

$$\hat{S}=\begin{pmatrix} r & t_{\|} & t_{\perp} & t_{\perp} \\ t_{\|} & r & t_{\perp} & t_{\perp} \\ t_{\perp} & t_{\perp} & r & t_{\|} \\ t_{\perp} & t_{\perp} & t_{\|} & r \end{pmatrix} \tag{39}$$

which corresponds to the most general form obeying time inversion and spacial D_4 dihedral symmetry, in combination with unitarity. The previous expressions involves three complex parameters, but as shown in Appendix A, unitarity leaves only three independent real variables. We have chosen the following parametrization:

$$\begin{aligned} r &= e^{i\psi}(e^{2i\phi_u}+e^{2i\phi_v}-2)/4, \\ t_{\|} &= e^{i\psi}(e^{2i\phi_v}+e^{2i\phi_u}+2)/4, \\ t_{\perp} &= e^{i\psi}(e^{2i\phi_v}-e^{2i\phi_u})/4, \end{aligned} \tag{40}$$

where $\phi_{u,v}\in[0,\pi[$ and $\psi\in[0,2\pi[$. Note that two lines in the (ϕ_u,ϕ_v) plane are especially interesting:

$$\phi_u=\pi/2 \Rightarrow t_{\perp}=t_{\|} \quad \text{(symmetric case)}$$

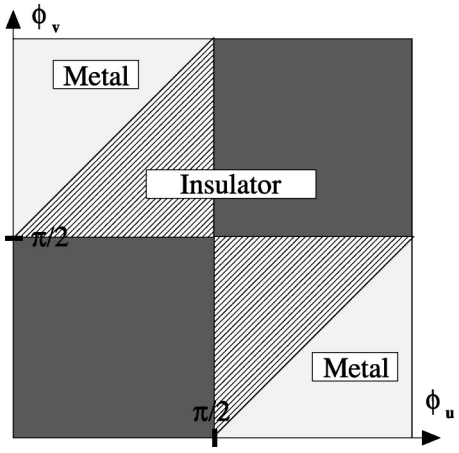

FIG. 4. Phase diagram for a noninteracting electron wire square grid. Contrary to the one-dimensional case, there are metallic states at integer filling factors for some values of the $\hat{S}$ matrix. In these regions of the phase diagram, the single electron spectrum is gapless.

$$\phi_u=\phi_v \Rightarrow t_{\perp}=0 \quad \text{(1D case)}. \tag{41}$$

A. Band structure

The derivation of the band structure is standard, so it is outlined in Appendix B. This band structure is given by an implicit equation:

$$x(k,\mathbf{k}')+y(k,\mathbf{k}')=\beta\equiv\frac{2\cos\phi_v}{\sin(\phi_u-\phi_v)}, \tag{42}$$

where

$$x(k,\mathbf{k}')\equiv\frac{\sin(ka+\psi)}{\cos\phi_u\cos(k'_x a)-\cos(ka+\psi+\phi_u)}, \tag{43}$$

$$y(k,\mathbf{k}')\equiv\frac{\sin(ka+\psi)}{\cos\phi_u\cos(k'_y a)-\cos(ka+\psi+\phi_u)}. \tag{44}$$

As usual, the energy of these states is given by the free electron dispersion $E_0(k)=\hbar^2k^2/(2m)$. Here, $\mathbf{k}'$ is the two-dimensional lattice wave vector, such that $\Psi(\mathbf{r}+\mathbf{R})=\exp(i\mathbf{k}'.\mathbf{R})\Psi(\mathbf{r})$ for any $\mathbf{r}$ on the wire network and any period $\mathbf{R}$ of the square lattice.

As we found some interesting features in the band structure of noninteracting electrons in a two-dimensional square grid we will describe it more precisely. Contrary to one dimension, there are values of the scattering matrix, for which the single electron spectrum is no longer gapped, and these are located in Fig. 4. More precisely, in the clear regions of Fig. 4, the single particle spectrum is gapless. In the dark regions, it is gapped, leading to an insulator if the electronic density corresponds to filling an *even integer* number of bands. Finally, in the dashed regions, we obtain an insulator for an *odd integer* number of bands.

We still have a 2π periodic structure in ka, but the band-structure consists of two types of foils: normal and abnormal.

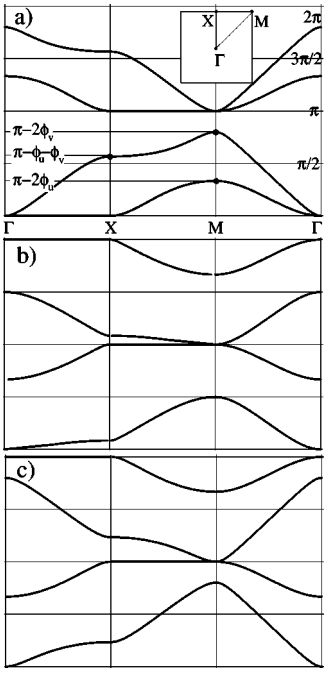

FIG. 5. Three characteristic band structure pictures for different values of the $\hat{S}$ matrix: (a) Insulator, $0<\phi_u,\phi_v<\pi/2$ (dark in Fig. 4); (b) insulator, $0<\phi_u<\pi/2, \pi/2<\phi_v<\pi, |\phi_u-\phi_v|<\pi/2$ (dashed line in Fig. 4); (c) conductor, $0<\phi_u<\pi/2, \pi/2<\phi_v<\pi, |\phi_u-\phi_v|>\pi/2$ (clear line in Fig. 4). The band structure is 2π periodic in k, and has four foils: two normal and two abnormal. Some foils are described as "abnormal" because of their strange curvature, revealed here by the flat part of these bands. Given the energy interval $0<k<\pi$ one could obtain the $\pi<k<2\pi$ interval by exchanging Γ and M points.

Normal bands resemble an ordinary band of a tight-binding model of square lattice crystal (a sort of deformed paraboloid). Abnormal bands are so called for their strange curvature. To get an idea of their form one could imagine a square rubber foil, attach its four extremities and then put inside a heavy cross. For a complete description, we give sections of the band structure in several directions for three characteristic values of the scattering matrix. Because of some important symmetries, we may restrict the domain of variation of $\{\phi_u,\phi_v\}$, and still get all the possible different physical pictures:

(1) $k(\phi_u,\phi_v)=k(\phi_v,\phi_u)$,

(2) $k(\pi-\phi_v,\pi-\phi_u)=-k(\phi_u,\phi_v)$.

These may be easily seen from form II of the dispersion relation, given in Appendix B. Both of them are reflection symmetries. Given the band structure for $k\in[0,\pi]$ and using the following symmetry: $k(k'_x,k'_y)+\pi=k(k'_x+\pi,k'_y+\pi)$, we easily expand it to the full interval $k\in[0,2\pi]$ by replotting the same band originating from point M instead of Γ (see Fig. 5).

B. RGF equation for a two-dimensional grid

Following the same procedure as in the one-dimensional case, we first calculate Hartree and exchange contributions to single electron energy and then establish the equivalent of Eq. (17) or Eq. (37) for two dimensions and finally get the RGF equation. The main difference with the 1D case is that we have now three real parameters for the $\hat{S}$-matrix and electron-electron interactions should be evaluated along two perpendicular threads that form our grid. The condition to satisfy now reads:

$$\frac{\partial E_0}{\partial \psi}\overline{\psi}(\Lambda)+\frac{\partial E_0}{\partial \phi_u}\overline{\phi}_u(\Lambda)+\frac{\partial E_0}{\partial \phi_v}\overline{\phi}_v(\Lambda) = \mathcal{E}_1(\hat{S}_0,\mathbf{k}',\Lambda_0)-\mathcal{E}_1(\hat{S}_0,\mathbf{k}',\Lambda). \quad (45)$$

As was proven in the previous section all networks with links of equal length are renormalizable, i.e., there is a set of functions $\overline{\phi}_u$, $\overline{\phi}_v$, and $\overline{\psi}$ depending only on Λ. Indeed the decomposition of the rhs of Eq. (45) on a basis of three functions depending on $\mathbf{k}'$ is possible. The corresponding renormalization group flow equations are

$$\frac{d\phi_u}{dl}=\frac{\alpha}{8}[\sin 2\phi_v+3\sin 2\phi_u+\sin 2(\phi_v-\phi_u)], \quad (46)$$

$$\frac{d\phi_v}{dl}=\frac{\alpha}{8}[\sin 2\phi_u+3\sin 2\phi_v+\sin 2(\phi_u-\phi_v)], \quad (47)$$

where $\alpha=U_0/(2\pi\hbar v_F)$. The only fixed points are $\phi_{u,v}=0,\pi/2$, among which there is only one attractor for $\{\phi_u,\phi_v\}=\{\pi/2,\pi/2\}$. The global behavior of this flow is illustrated in Fig. 6. These properties of the RGF for a single node connecting four semi-infinite wires have already been described by Lal *et al.*[32] and Das *et al.*[35] As for the one-dimensional example of Sec. II above, the new feature associated to a regular lattice is the presence of commensurability effects. We have to stop the renormalization procedure when all the completely filled bands have been eliminated. From Fig. 5, we expect to obtain one or two partially filled bands crossing the Fermi level. These bands are only very weakly dispersive, since the effective $\hat{S}$ matrix for the nodes is then very close to its value at the vanishing transmission fixed point. Suppose now that this fixed point is approached from

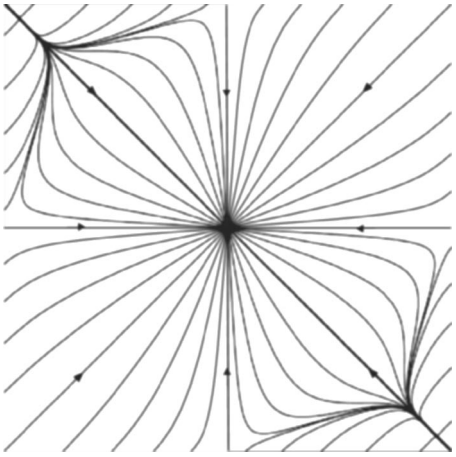

FIG. 6. RGF for the 2D square grid of wire. The only attractor is in the picture center for $\{\phi_u,\phi_v\}=(\pi/2,\pi/2)$.

the dark regions of the phase diagram shown in Fig. 4. If the filling factor corresponds to an *even integer*, the Fermi level lies in a gap of the renormalized band structure. Therefore, we may eliminate the remaining pair of filled bands, and the system is an insulator. Similarly, a true insulator is obtained for an *odd integer* filling factor, in the case where the $(\pi/2,\pi/2)$ fixed point is approached from the dashed regions in Fig. 4. Experimentally, one expects transitions between these commensurate insulators and strongly renormalized "heavy electron" metals at generic filling factors if the electronic density is controlled by a uniform external gate voltage.

Another interesting feature of this geometry is the fact that the flow may induce metal-insulator transitions for some commensurate filling factors at a *finite* energy scale. Indeed, for initial parameters lying in the clear regions of Fig. 4, corresponding to a gapless single electron spectrum, Fig. 6 shows that the system always reaches either the dashed or dark regions in a finite RG time. Experimentally, these RG flows may be visualized by gradually lowering the temperature, since at least qualitatively, the energy scale set by temperature plays the role of the moving cut-off Λ.

V. CONCLUSION

In this paper, we have studied a particular class of networks of Luttinger liquids, with nodes connected by links of a constant length. In the limit of long links, compared to the Fermi wavelength, we studied the evolution of the scattering matrix at the nodes, as the typical energy scale for the occupied states contributing to Friedel oscillations is getting closer to the Fermi level. The corresponding renormalization group flow turns to be identical to the one already found for a single node coupled to several semi-infinite 1D Luttinger liquids.[32] This result is physically reasonable, since we have considered the limit of long links. However, we emphasize that these renormalization effects come from quasiparticle scattering on Friedel oscillations induced by the nodes, which are a rather complicated function of the lattice geometry. For instance, even in the limit of very long links, the amplitudes A_{ij} which determine the value of energy eigenfunctions along the links are obtained from a $2N_L \times 2N_L$ eigenvalue problem whose solution has a strongly nonlocal character.

The main difference between a regular lattice and a simple node coupled to infinite wires is that in the former case, we have to stop the renormalization procedure when the last occupied band has been integrated out. So instead of having completely disconnected wires in the low-energy limit, we expect in general a strongly renormalized conducting system with an effective Fermi velocity much reduced in comparison to a noninteracting system with the same density. These effects should be visible as a power-law behavior of the network conductance as a function of temperature. Insulating ground states are expected when the electronic density corresponds to filling some integer numbers of bands.

Of course, this work leaves many open questions. It would be interesting to generalize the present renormalization approach to lattices containing links with several different lengths. In such situations, the spectrum no longer exhibits a simple periodic structure, and some signatures of quantum chaos, already manifested in the single particle density of states,[46] may also appear in the temperature dependence of the conductivity of an interacting system. Another open question is the influence of an external magnetic field, which also drastically modifies the single-particle spectrum. Finally, the limit of strong electron-electron interaction deserves further investigation, and in particular the possibility to develop some new metal-insulator transitions for noninteger but rational filling factors, generalizing the notion of a Wigner crystal. Such insulating states would naturally be pinned by the nodes of the lattice.

ACKNOWLEDGMENTS

We would like to thank J. Dufouleur, G. Faini, D. Mailly, C. Naud, and J. Vidal for interesting discussions on various aspects of conducting wire networks.

APPENDIX A: PARAMETRIZATION OF THE $\hat{S}$ MATRIX

In this appendix we will show that time-inversion, spacial D_4 dihedral symmetry combined with unitarity imply a parameterization of scattering matrix in terms of three real variables. For a two-dimensional square lattice, the most general form of the $\hat{S}$ matrix is given by a 4×4 matrix:

$$\begin{pmatrix} A' \\ B' \\ C' \\ D' \end{pmatrix} = \begin{pmatrix} r_A & t_{BA} & t_{CA} & t_{DA} \\ t_{AB} & r_B & t_{CB} & t_{DB} \\ t_{AC} & t_{BC} & r_C & t_{DC} \\ t_{AD} & t_{BD} & t_{CD} & r_D \end{pmatrix} \begin{pmatrix} A \\ B \\ C \\ D \end{pmatrix}, \tag{A1}$$

where A, B, C, D are the coefficients of incoming plane waves. Primed values denote coefficients of outgoing waves. At this stage, one has 16 complex parameters for this $\hat{S}$-matrix.

Unitarity condition ($\hat{S}^\dagger\hat{S}=I$) combined with time-inversion symmetry ($\hat{S}^{-1}=\hat{S}^*$) gives $\hat{S}^t=\hat{S}$ (notice that $\hat{S}^t$ is the transposed matrix, not the conjugate). It leaves 10 complex parameters. Using four reflections of two types (1) $A\leftrightarrow B$, and (2) $A\leftrightarrow C$, $B\leftrightarrow D$ that generate the dihedral symmetry group D_4 consequently reduces this number to three complex variables. We obtain the $\hat{S}$-matrix in the form (39). Unitarity allows finally to express the scattering matrix with only 3 real parameters:

$$|r|^2 + 2|t_\perp|^2 + |t_\parallel|^2 = 1,$$

$$rt_\perp^* + r^* t_\perp + t_\perp^* t_\parallel + t_\parallel^* t_\perp = 0,$$

$$rt_\parallel^* + r^* t_\parallel + 2|t_\perp|^2 = 0.$$

Subtracting the third equation from the first one allows us to define a first real parameter ψ:

$$|r - t_\parallel| = 1 \Rightarrow r = t_\parallel - e^{i\psi}.$$

There remains two independent equations:

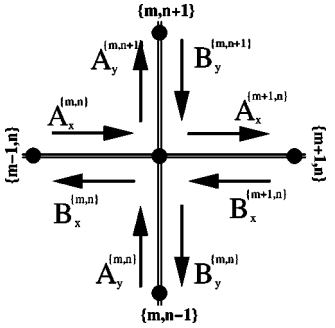

FIG. 7. In the 2D case, each node is indexed by a pair of numbers $\{m,n\}$. Incoming and outgoing plane waves are connected by the 4×4 scattering matrix.

$$2(|t_{\|}|^2+|t_{\perp}|^2)=t_{\|}e^{-i\psi}+t_{\|}^{*}e^{i\psi}, \quad \text{(I)}$$

$$2(t_{\perp}^{*}t_{\|}+t_{\perp}t_{\|}^{*})=t_{\perp}e^{-i\psi}+t_{\perp}^{*}e^{i\psi}, \quad \text{(II)}$$

$$2|t_{\|}+t_{\perp}|^2=2\,\mathrm{Re}[(t_{\|}+t_{\perp})e^{-i\psi}], \quad \text{(I}-\text{II)}$$

$$2|t_{\|}-t_{\perp}|^2=2\,\mathrm{Re}[(t_{\|}-t_{\perp})e^{-i\psi}]. \quad \text{(I}+\text{II)}.$$

Two more real parameters are needed to complete the parametrization:

$$t_{\|}-t_{\perp}=\cos\phi_u e^{i(\phi_u+\psi)},$$

$$t_{\|}+t_{\perp}=\cos\phi_v e^{i(\phi_v+\psi)}.$$

Expressions of transmission and reflection coefficients as functions of these three three real parameters are given in the main text, see Eq. (40). We remark on an interesting fact: in the case of perfect transmission ($r=0$), only the separate thread solution ($|t_{\|}|=1, t_{\perp}=0$) is possible.

APPENDIX B: BAND STRUCTURE FOR A SQUARE LATTICE OF WIRES

In this appendix we derive the band structure for a square lattice of wires of noninteracting electrons. As in the one-dimensional case, the wave function away from impurities (i.e., nodes here) could be written as combination of plane waves:

$$\psi_k(x)=A_i^{m,n}e^{ikx}+B_i^{m,n}e^{-ikx}, \quad \text{(B1)}$$

where $i=\{x,y\}$ and the coefficients $\{A_x^{m,n},A_y^{m,n},B_x^{m,n},B_y^{m,n}\}_{m,n}$ are defined in Fig. 7. By definition of the scattering matrix:

$$\begin{pmatrix} B_x^{m,n} \\ A_x^{m+1,n} \\ A_y^{m,n+1} \\ B_y^{m,n} \end{pmatrix} = \hat{S}\begin{pmatrix} A_x^{m,n} \\ B_x^{m+1,n} \\ B_y^{m,n+1} \\ A_y^{m,n} \end{pmatrix} = \begin{pmatrix} r & t_{\|} & t_{\perp} & t_{\perp} \\ t_{\|} & r & t_{\perp} & t_{\perp} \\ t_{\perp} & t_{\perp} & r & t_{\|} \\ t_{\perp} & t_{\perp} & t_{\|} & r \end{pmatrix}\begin{pmatrix} A_x^{m,n} \\ B_x^{m+1,n} \\ B_y^{m,n+1} \\ A_y^{m,n} \end{pmatrix}, \quad \text{(B2)}$$

Bloch periodicity condition for the wave function implies

$$A_x^{n,m}=e^{i(k_x'-k)na}e^{ik_y'ma}A_x^{0,0},$$

$$B_x^{n,m}=e^{i(k_x'+k)na}e^{ik_y'ma}B_x^{0,0},$$

$$A_y^{n,m}=e^{i(k_y'-k)ma}e^{ik_x'na}A_y^{0,0},$$

$$A_x^{n,m}=e^{i(k_y'+k)ma}e^{ik_y'na}B_y^{0,0}. \quad \text{(B3)}$$

Using the last two expressions, we obtain the secular equation:

$$\begin{vmatrix} t_{\|}e^{i(k-k_x')a}-1 & re^{2ika} & t_{\perp}e^{i(k-k_x')a} & t_{\perp}e^{i(k_y'-k_x'+2k)a} \\ r & t_{\|}e^{i(k_x'+k)a}-1 & t_{\perp} & t_{\perp}e^{i(k_y'+k)a} \\ t_{\perp}e^{i(k-k_y')a} & t_{\perp}e^{i(k_x'-k_y'+2k)a} & t_{\|}e^{i(k-k_y')a}-1 & re^{2ika} \\ t_{\perp} & t_{\perp}e^{i(k_x'+k)a} & r & t_{\|}e^{i(k_y'+k)a}-1 \end{vmatrix} = 0. \quad \text{(B4)}$$

Replacing scattering matrix elements by their parametrization (40), we get the implicit band-structure equation given in the main text (43). Here we propose two more different ways to write the same dispersion relation, where the combinations $ka+\psi$, $k_x'a$ and $k_y'a$ have been replaced, respectively, by the simpler notations k, k_x', and k_y':

$$\cos(k+\phi_u)\cos(k+\phi_v)+\cos k_x'\cos k_y'\cos\phi_u\cos\phi_v \quad \text{(I)}$$
$$=\tfrac{1}{2}(\cos k_x'+\cos k_y')$$
$$\times[\cos\phi_u\cos(k+\phi_v)+\cos\phi_v\cos(k+\phi_u)]$$

$$\frac{\cos(k+\phi_u)-\cos\phi_u\cos k_x'}{\cos(k+\phi_u)-\cos\phi_u\cos k_y'} = -\frac{\cos(k+\phi_v)-\cos\phi_v\cos k_x'}{\cos(k+\phi_v)-\cos\phi_v\cos k_y'}. \quad \text{(II)}$$

The first form is useful to identify symmetries of band structure. The second form is useful to derive RGF equations directly without using the formalism developed in Sec. III. We remark that in the 1D case ($t_{\perp}=0$), and in the 2D symmetric case ($t_{\perp}=t_{\|}$) the band structure equations are the same, namely, $\cos(ka+\psi+\phi)=\cos\phi\cos(k'a)$.

APPENDIX C: ANY LATTICE GENERALIZATION

In this part we will discuss particular points met in Sec. III of this article. First of all we could obtain the dispersion relation for any network, i.e., when the wires lengths are not necessarily equal. In that case Eq. (25) is modified into

$$A_{ij}=\sum_m{}^{(j)}e^{ikL_{ij}/2}S_{im}^{(j)}e^{ikL_{jm}/2}A_{jm}. \quad \text{(C1)}$$

We choose the origin of coordinates needed to define the amplitudes A_{ij} at the centers of each link. This formula means that the amplitude of the wave going from node j to node i is the sum of amplitudes coming from all neighbors m of node j, multiplied by phase factors $\exp(ikL_{jm}/2)$ due to

propagation from the middle of link $\langle jm\rangle$ to the node j, then scattered on node j with probability amplitude $S_{im}^{(j)}$ and finally reaching the middle of link $\langle ij\rangle$ with a new phase factor $\exp(ikL_{ij}/2)$. We will now write the same equation in vector form. The expression will be more transparent and this permits us to express the secular equation for energy eigenvalues k in a compact form. If we fix the energy of the system then the stationary states are completely determined by $2N_L$ amplitudes, where N_L is the number of links. The factor 2 arises since each wave can propagate in two opposite directions on each link. So the set of amplitudes $\{A_{ij}\}$ could be presented as a vector $|A\rangle$ in a $2N_L$-dimensional Hilbert space. We choose the orthonormal basis associated with network links $\langle mn|ij\rangle = \delta_{mi}\delta_{nj}$. Each link is represented by two basis vector $|ij\rangle$ and $|ji\rangle$, this orientation difference should be taken into account in various summations over first neighbors. We define the vector $|A\rangle = \Sigma_{\langle ij\rangle} A_{ij}|ij\rangle$ and the length operator $\hat{L} = \Sigma_{\langle ij\rangle} L_{ij}|ij\rangle\langle ij|$. The vector form of Eq. (C1) reads

$$|A(k)\rangle = e^{ik\hat{L}/2}\hat{T}e^{ik\hat{L}/2}|A(k)\rangle. \tag{C2}$$

The possible values of k are given by

$$\det(e^{-ik\hat{L}} - \hat{T}) = 0. \tag{C3}$$

One remarks that the periodicity of the spectrum (28) is lost in the general case, unless there exists a Δk such that $\exp(i\Delta k\hat{L}) = 1$. Let us be reminded that this periodicity of the spectrum allowed us to evaluate the integral $I(k)$ in Eq. (31): the contribution of each band was the same and we replaced the sum over any filled band just by sum over all the eigenvectors of operator $\hat{T}$.

The second point to be clarified is the spectral decomposition $\Sigma_q |q\rangle e^{-iqa}\langle q| = \hat{T}$. It holds only if $|q\rangle$ vectors form an orthonormal basis. Orthogonality is clear as $|q\rangle$ is an eigenvector of a unitary operator,

$$\langle q|\hat{T}|k\rangle = e^{-iqa}\langle q|k\rangle = e^{-ika}\langle q|k\rangle. \tag{C4}$$

Let us now evaluate the vector norm in the $|ij\rangle$ basis:

$$\langle q|q\rangle = \sum_{\langle ij\rangle} \langle q|ij\rangle\langle ij|q\rangle = \sum_{\langle ij\rangle} |A_{ij}(q)|^2. \tag{C5}$$

But we know that the norm of wave function (24) in the physical Hilbert space should be equal to unity.

$$\int_{\text{network}} |\psi(x)|^2 dx = 1 = a\sum_{\langle ij\rangle} \left(|A_{ij}(q)|^2 + A_{ij}(q)A_{ji}^*(q)\frac{\sin(ka)}{ka}\right). \tag{C6}$$

So if we demand $\langle q|q\rangle = 1$ we are doing an approximation neglecting the term proportional to $\sin(ka)/ka$. This approximation is legitimate in our case, as we consider systems where the typical number ef electrons along each link between two nodes is large. Clearly, it will break down for links of the order of the Fermi wavelength. Supposing that $\langle q|q\rangle = 1$ is equivalent to identifying the norm in the (infinite dimensional) physical Hilbert space, with the norm associated with the orthonormal basis $|ij\rangle$ in the ($2N_L$ dimensional) auxiliary Hilbert space. The fact that our equations are not depending explicitly on the network scale parameter a is closely related to this approximation. So if one were to estimate finite size corrections to the RGF equation, one should take the physical normalization of the $|q\rangle$ basis into account. Such corrections would likely produce RGF equations where the nodes on the lattice are no longer renormalized independently of each other, by contrast to what we obtained in Sec. III; see Eq. (38).

[1] G. Timp, R. E. Behringer, E. H. Westerwick, and J. E. Cunningham, in *Quantum Coherence in Mesoscopic Systems*, edited by B. Kramer (Plenum, New York, 1991).

[2] S. Washburn and R. A. Webb, Rep. Prog. Phys. **55**, 1311 (1992).

[3] G. Timp, A. M. Chang, J. E. Cunningham, T. Y. Chang, P. Mankiewich, R. Behringer, and R. E. Howard, Phys. Rev. Lett. **58**, 2814 (1987).

[4] S. Pedersen, A. E. Hansen, A. Kristensen, C. B. Sorensen, and P. E. Lindelof, Phys. Rev. B **61**, 5457 (2000).

[5] D. Mailly, C. Chapelier, and A. Benoit, Phys. Rev. Lett. **70**, 2020 (1993).

[6] W. Rabaud, L. Saminadayar, D. Mailly, K. Hasselbach, A. Benoît, and B. Etienne, Phys. Rev. Lett. **86**, 3124 (2001).

[7] M. L. Roukes, A. Scherer, S. J. Allen, Jr., H. G. Craighead, R. M. Ruthen, E. D. Beebe, and J. P. Harbison, Phys. Rev. Lett. **59**, 3011 (1987).

[8] C. J. B. Ford, T. J. Thornton, R. Newbury, M. Pepper, H. Ahmed, D. C. Peacock, D. A. Ritchie, J. E. F. Frost, and G. A. C. Jones, Phys. Rev. B **38**, 8518 (1988).

[9] D. G. Ravenhall, H. W. Wyld, and R. L. Schult, Phys. Rev. Lett. **62**, 1780 (1989).

[10] G. Kirczenow, Phys. Rev. Lett. **62**, 2993 (1989).

[11] H. U. Baranger and A. D. Stone, Phys. Rev. Lett. **63**, 414 (1989).

[12] C. W. J. Beenakker and H. van Houten, Phys. Rev. Lett. **63**, 1857 (1989).

[13] C. J. B. Ford, S. Washburn, M. Büttiker, C. M. Knoedler, and J. M. Hong, Phys. Rev. Lett. **62**, 2724 (1989).

[14] C. Naud, G. Faini, and D. Mailly, Phys. Rev. Lett. **86**, 5104 (2001).

[15] J. Vidal, R. Mosseri, and B. Douçot, Phys. Rev. Lett. **81**, 5888 (1998).

[16] J. Vidal, G. Montambaux, and B. Douçot, Phys. Rev. B **62**, R16 294 (2000).

[17] M. Grayson, D. C. Tsui, L. N. Pfeiffer, K. W. West, and A. M. Chang, Phys. Rev. Lett. **80**, 1062 (1998).

[18] X. G. Wen, Phys. Rev. B **41**, 12 838 (1990).

[19] C. L. Kane and M. P. A. Fisher, Phys. Rev. Lett. **72**, 724 (1994).

[20] R. de-Picciotto, M. Reznikov, M. Heiblum, V. Umansky, G. Bunin, and D. Mahalu, Nature (London) **389**, 162 (1997).

[21] L. Saminadayar, D. C. Glattli, Y. Jin, and B. Etienne, Phys. Rev.

Lett. **79**, 2526 (1997).
[22] M. Bockrath, D. H. Cobden, J. Lu, A. G. Rinzler, R. E. Smalley, L. Balents, and P. L. McEuen, Nature (London) **397**, 598 (1999).
[23] Z. Yao, H. W. C. Postma, L. Balents, and C. Dekker, Nature (London) **402**, 273 (1999).
[24] R. Egger and A. O. Gogolin, Phys. Rev. Lett. **79**, 5082 (1997).
[25] C. Kane, L. Balents, and M. P. A. Fisher, Phys. Rev. Lett. **79**, 5086 (1997).
[26] C. Papadopoulos, A. Rakitin, J. Li, A. S. Vedeneev, and J. M. Xu, Phys. Rev. Lett. **85**, 3476 (2000).
[27] J. Kim, K. Kang, J.-O Lee, H.-H. Yoo, J.-R. Kim, J. W. Park, H. M. So, and J.-J. Kim, J. Phys. Soc. Jpn. **70**, 1464 (2001).
[28] M. Terrones, F. Banhart, N. Grobert, J.-C. Charlier, H. Terrones, and P. M. Ajayan, Phys. Rev. Lett. **89**, 075505 (2002).
[29] B. Gao, A. Komnik, R. Egger, D. C. Glattli, and A. Bachtold, cond-mat/0311645 (unpublished).
[30] A. Komnik and R. Egger, Phys. Rev. Lett. **80**, 2881 (1998).
[31] C. Nayak, M. P. A. Fisher, A. W. W. Ludwig, and H. H. Lin, Phys. Rev. B **59**, 15 694 (1999).
[32] S. Lal, S. Rao, and D. Sen, Phys. Rev. B **66**, 165327 (2002).
[33] S. Chen, B. Trauzettel, and R. Egger, Phys. Rev. Lett. **89**, 226404 (2002).
[34] C. Chamon, M. Oshikawa, and I. Affleck, Phys. Rev. Lett. **91**, 206403 (2003).
[35] S. Das, S. Rao, and D. Sen, cond-mat/0311563 (unpublished).
[36] R. L. Schult, H. W. Wyld, and D. G. Ravenhall, Phys. Rev. B **41**, 12 760 (1990).
[37] P. S. Deo and A. M. Jayannavar, Phys. Rev. B **50**, 11 629 (1994).
[38] S. Uryu and T. Ando, Phys. Rev. B **53**, 13 613 (1996).
[39] C. L. Kane and M. P. A. Fisher, Phys. Rev. Lett. **68**, 1220 (1992).
[40] C. L. Kane and M. P. A. Fisher, Phys. Rev. B **46**, 15 233 (1992).
[41] D. Yue, L. I. Glazman, and K. A. Matveev, Phys. Rev. B **49**, 1966 (1994).
[42] V. Meden, W. Metzner, U. Schollwöck, and K. Schönhammer, Phys. Rev. B **65**, 045318 (2002).
[43] V. Meden, W. Metzner, U. Schollwöck, and K. Schönhammer, J. Low Temp. Phys. **126**, 1147 (2002).
[44] V. Meden, S. Andergassen, W. Metzner, U. Schollwöck, and K. Schönhammer, Europhys. Lett. **64**, 769 (2003).
[45] P. W. Anderson, J. Phys. C **3**, 2346 (1970).
[46] T. Kottos and U. Smilansky, Phys. Rev. Lett. **79**, 4794 (1997).
[47] R. L. Schult, D. G. Ravenhall, and H. W. Wyld, Phys. Rev. B **39**, 5476 (1989).
[48] K.-F. Berggren and Z.-L. Ji, Phys. Rev. B **43**, 4760 (1991).